*fermentation*

MDPI

*Article*

# Anti-Osteoporotic Activity of *Pueraria lobata* Fermented with *Lactobacillus paracasei* JS1 by Regulation of Osteoblast Differentiation and Protection against Bone Loss in Ovariectomized Mice

**Seon Yu Kim [1,†], Hee-Ju Lee [1,†], Taehyun Kim [1,†], Yeong-Geun Lee [1], Jeong Eun Kwon [1,*] and Se Chan Kang [1,2,*]**

[1] Department of Biotechnology, Kyung Hee University, Yongin 17104, Korea; sykim@nmr.kr (S.Y.K.); leeheeju815@gmail.com (H.-J.L.); silsoo96@naver.com (T.K.); lyg629@nate.com (Y.-G.L.)
[2] Mbiometherapeutics Co., Ltd., Yongin 16942, Korea
* Correspondence: jjung1169@khu.ac.kr (J.E.K.); sckang@khu.ac.kr (S.C.K.); Tel.: +82-31-201-5636 (J.E.K.); +82-31-201-2687 (S.C.K.)
† These three authors contributed equally to this work.

**Abstract:** Osteoporosis is the most common bone disease associated with low bone mineral density. It is the process of bone loss and is most commonly caused by decreased estrogen production in women, particularly after menopause. *Pueraria lobata,* which contains various metabolites, especially isoflavone, is widely known as regulator for bone mineral contents. In this study, the effects of the *P. lobata* extract (PE) with or without fermentation with *Lactobacillus paracasei* JS1 (FPE) on osteoporosis were investigated in vitro and in vivo. The effects of PE and FPE on human osteoblastic MG63 cells, RAW 264.7 cells, and ovariectomized (OVX)-induced model mice were analyzed at various ratios. We found that FPE increased calcium deposition and inhibited bone resorption by in vitro assay. Furthermore, treatment with PE and FPE has significantly restored destroyed trabecular bone in the OVX-induced bone loss mouse model. Overall, FPE demonstrated bioactivity to prevent bone loss by decreasing bone turnover.

**Keywords:** fermentation; *Lactobacillus*; *Pueraria lobata*; osteoblast; ovariectomized-induced model



**Citation:** Kim, S.Y.; Lee, H.-J.; Kim, T.; Lee, Y.-G.; Kwon, J.E.; Kang, S.C. Anti-Osteoporotic Activity of *Pueraria lobata* Fermented with *Lactobacillus paracasei* JS1 by Regulation of Osteoblast Differentiation and Protection against Bone Loss in Ovariectomized Mice. *Fermentation* **2021**, *7*, 186. https://doi.org/10.3390/fermentation7030186

Academic Editor: Hiroshi Kitagaki

Received: 30 July 2021
Accepted: 6 September 2021
Published: 9 September 2021



## 1. Introduction

Isoflavones found in soybeans are nonsteroidal, phytoestrogenic, and anti-oxidative compounds with potential roles in the prevention of chronic diseases, including hormone-dependent diseases, cardiovascular diseases, breast and prostate cancer, osteoporosis, and postmenopausal symptoms [1]. For example, the efficacy of isoflavone derivatives such as dihydrodaidzein (DHD) and equol (EQ) have been evaluated against various hormone-dependent diseases due to their strong binding affinity for estrogen receptors.

Osteoporosis is a bone disease characterized by the destruction of bone tissue, loss of bone mass, and an increased risk of bone fractures [2–4]. Osteoporosis can be classified as primary or secondary depending on its cause. Primary osteoporosis induced by menopause causes a rapid decrease in estrogen levels; leads to the activation of osteoclasts, the cells involved in bone resorption; and imparts the inactivation of osteoblasts, the cells involved in bone formation [5]. When the balance between osteoblasts and osteoclasts is lost, bone resorption is promoted, bone turnover rate is increased, and bone mineral density is lowered, leading to increased fracture and osteoporosis [6]. Secondary osteoporosis is usually caused by other medical conditions or treatments that interfere with the attainment of peak bone mass and may cause bone loss. These medical conditions include genetic diseases, serious kidney failure, rheumatoid arthritis, chronic obstructive pulmonary diseases, endocrine disorders, nutritional imbalance, inflammatory disease, and drug abuse [7–9].

Treatment of osteoporosis generally involves anti-resorptive and anabolic medications in combination with calcium and vitamin D supplementation. With respect to anti-resorptive drugs, bisphosphonates and calcitonin are the most commonly used for the treatment of postmenopausal osteoporosis [10,11]. Regarding anabolic drugs, human parathyroid hormone analogs promote osteoblast formation [12,13]. Selective estrogen receptor modulators (SERMs) improve bone mineral density (BMD) via the mechanisms of hormone replacement therapy; however, side effects have been reported, including increased risk of stroke and venous thromboembolism [12]. Aside from conventional drug therapy, alternative treatments such as traditional medicine are also used to mitigate osteoporosis. Natural products, especially herbal medicine, have received growing attention in the prevention of osteoporosis. For instance, flavonoids derived from *Epimedium brevicornum* Maxim have been proven to improve estrogen deficiency-induced osteoporosis in ovariectomized rats via direct osteoblast stimulation and inhibition of bone resorption, leading to an overall anabolic effect on periosteum and trabecula [10].

Likewise, isoflavones have been demonstrated as valuable for attenuating menopause-induced osteoporotic bone loss by regulating bone-related factors [14]. *Pueraria lobata*, which is known for its main bioactive components, isoflavones, is a perennial vine native to Asia and primarily subtropical and temperate regions of China, Japan, and Korea. The starch extracted from its roots is used in cooking and herbal medicines [15,16] in a wide variety of applications. Recent research has focused on its antidipsotropic activity for the treatment of alcohol-related health effects [17]. Furthermore, *P. lobata* has demonstrated antioxidant, anti-diabetic, and anti-inflammatory activity [18–21]. With strong applicability to the treatment of osteoporosis, *P. lobata* has been reported to regulate receptor activator of nuclear factor kappa-B ligand (RANKL)-mediated osteoclastogenesis [22], proliferation, differentiation, and mineralization [23]. To enhance the efficacy of *P. lobata*, bioconversion with *Lactobacillus paracasei* JS1 was performed.

*Lactobacillus paracasei* JS1 is a gram-positive, non-spore-forming microorganism and lactic acid bacterium that is commonly used in dairy product fermentation and probiotics [24]. *L. paracasei* has been isolated from the healthy gastrointestinal tract and human feces [25]. In our previous study, *L. paracasei* JS1 showed an inhibitory effect on cytokine-mediated inflammation in the large intestine, as well as has beneficial effects on the skin due to its ability to produce equol [26]. Thus, it was hypothesized that *L. paracasei* JS1 could be effective in the prevention of osteoporosis, which has a strong relationship with estrogen deficiency. Here, we evaluated the efficacy of the *L. paracasei* JS1-induced fermentation products of *P. lobata* (FPE) which contain various flavonoids, in the prevention of osteoporosis. The efficacies of DHD and EQ, which are derivatives of FPE, and 17$\beta$-estradiol ($E_2$) were compared with the efficacy of FPE.

## 2. Materials and Methods

### *2.1. Sample Preparation*

*P. lobata* roots were provided by Professor Tae-Ho Park from the green-house at Daegu University (Daegu, Korea). A voucher specimen (KHU-BMRI-PL-2016) was deposited in the Biomedical Research Institute of Kyung Hee University. *P. lobata* roots were chopped into small pieces and extracted three times in 30% ethanol for 24 h at room temperature, respectively. The extract was subsequently filtered to remove any particulates and concentrated in vacuo. Then, the concentrated crude extract was lyophilized to obtain a powder and stored at −20 °C for subsequent experimentation. Consequently, the yield of PE was 13.2% and FPE was 4.4%, respectively.

### *2.2. Bacterial Culture and Fermentation*

To discover an ideal growth condition, *L. paracasei* JS1 was incubated at various conditions. The bacteria were incubated at 37 °C for 72 h with various speeds of agitation.

The isoflavone contents were measured by high-performance liquid chromatography (HPLC). It turned out that incubation at 37 °C for 72 h with an agitation speed of 250 rpm

was the most optimal growth condition, resulting in the most isoflavone content out of all other investigated agitation speeds (data not shown). For the preparation of *P. lobata* fermentation extract (FPE), *L. paracasei* JS1 was cultured in a liquid Gifu anaerobic medium (GAM) under aerobic conditions with 2% *P. lobata* extract at 37 °C for 72 h and an agitation speed of 250 rpm.

### *2.3. Metabolite Profiling of FPE Using Liquid Chromatography-Mass Spectrometry Analysis*

Liquid chromatography-mass spectrometry (LC-MS) analysis was performed using a SCIEX Triple TOF 5600 (SCIEX, Framingham, MA, USA) operating positive ion mode. Mass spectrometry was performed in the MSE acquisition mode, which enabled alternation between high- and low-energy scans. The operating parameters were set as follows: MS scan type, full scan and information dependent acquisition scanning; ionization source, electrospray ionization (ESI); MS scan range, $m/z$ 100 to 2000; MS/MS scan range, $m/z$ 30 to 2000; nebulizing gas, 50 psi; heating gas, 50 psi; curtain gas, 25 psi; desolvation temperature, 500 °C; ion spray voltage floating, 5.5 kV; declustering potential, 60 V; collision energy, 10 V; cone voltage, 35 ± 15 V.

### *2.4. Cell Culture*

Human MG63 cells, obtained from American Type Culture Collection (ATCC, Manassas, VA, USA) were cultured in alpha-MEM supplemented with 10% fetal bovine serum (FBS) and 1% penicillin and streptomycin (P/S).

Mouse macrophage RAW 264.7 cells purchased Korean Cell Line Bank (KCLB, Seoul, Korea) were cultured in DMEM supplemented with 10% FBS and 1% P/S. Cells were incubated at 37 °C and 5% $CO_2$ in a humidified atmosphere.

### *2.5. Osteoblast Proliferation Assay*

MG63 cell proliferation was evaluated using the MTT assay. Cells were seeded at $2 \times 10^4$ cells per well in 96-well plates. After 24 h of incubation, the cells were washed with phosphate-buffered saline (PBS) and cultured in MEM containing the indicated concentrations of PE, FPE, DHD, or EQ (0.01, 0.1, 1, 10, or 100 μg/mL final concentrations), respectively. After 72 h of incubation, the MTT solution in PBS was added to a final concentration of 0.5 mg/mL, followed by incubation for 4 h at 37 °C. At the end of 4 h of incubation, the supernatant medium was removed. Cell suspension in 100 μL of DMSO was subsequently performed. Absorbance was measured at 540 nm using a microplate reader (Tecan, Mannedorf, Switzerland). Cell proliferation rates were calculated from the OD readings and reported as percentages of vehicle control.

### *2.6. Alkaline Phosphatase Assay*

MG63 cells were maintained in a complete medium. Cells were seeded at $2 \times 10^4$ cells per well in 24-well plates. The medium was changed to a differentiation medium consisting of 10 mM glycerol 2-phosphate, 50 μg/mL ascorbic acid, and the indicated concentrations of PE, FPE, DHD, EQ, or $E_2$ (0.01, 0.1, 1, 10, or 100 μg/mL final concentrations) in culture medium after 24 h of incubation. After 96, 120 h of treatment, the cells were washed with PBS, and assay buffer was added. The solution was centrifuged at 12,000 rpm for 15 min at 4 °C. The supernatant was transferred to 96-well plates, and 5 mM pNPP solution was subsequently added after incubation for 1 h at 25 °C. The reaction was stopped by adding a stop solution, and the absorbance was measured at 405 nm. ALP activity was presented as a percentage, which was compared with ALP activity in control cells.

### *2.7. Real-Time PCR*

Total RNA was extracted using the TRizol reagent (Thermo Fisher Scientific, Waltham, MA, USA) according to the manufacturer's protocols after 72 h of incubation. The expression of osteoporosis-related genes in MG63 cells was detected by real-time quantitative PCR using SYBR Green technology. For each RNA sample, the expression of $\beta$-actin was

quantified by RT-PCR. The differential gene expression between samples was also estimated using the CT method. The primer sequences were obtained from Takara (Kyoto, Japan). All target gene-specific primer sequences are listed in Table 1.

**Table 1.** Target gene-specific primer sequences.

| Target Genes | 5′ to 3′ | Sequence |
|---|---|---|
| RANKL | Forward | ATGGCGTCCTCTCTGCTTG |
| | Reverse | TGAAAGGTCAGCGTATGGCTT |
| Runx2 | Forward | CCGGTCTCCTTCCAGGAT |
| | Reverse | GGGAACTGCTGTGGCTTC |
| Osteocalcin | Forward | CCGGTCTCCTTCCAGGAT |
| | Reverse | GGGAACTGCTGTGGCTTC |
| Osterix | Forward | ATGGCGTCCTCTCTGCTTG |
| | Reverse | TGAAAGGTCAGCGTATGGCTT |
| β-actin | Forward | CGCTGATGCATGCCTATGA |
| | Reverse | AGAGGTCCACAGAGCTGATTCC |

### *2.8. Osteoclast Differentiation Assay*

RAW 264.7 cells were cultured to $2 \times 10^4$ cells per well in 24-well plates. After 24 h of incubation, the cells were washed with PBS and cultured for 5 days after treatment with 50 ng/mL of RANKL and 30 ng/mL of M-CSF (Peprotech, Rocky Hill, NJ, USA). After treatment with R/M, 100 μg/mL of PE and FPE, 10 μg/mL of DHD and EQ, and $10^{-9}$ M of $E_2$ were added, and the cells were incubated for 48 h at 5% $CO_2$ and 37 °C, respectively. Out of the osteoclast population, TRAP-positive multinucleated cells (MNCs) with more than three nuclei were measured using the Acid Phosphatase Leukocyte (TRAP) Kit (Sigma-Aldrich, St.Louis, MA, USA). The cells were removed by washing with PBS, and then each well was photographed by a microspore camera (Tecan).

### *2.9. Animals*

Female 6-week-old outbred ICR mice were purchased from RaonBio Co., Ltd. (Yongin, Korea) and were surgically ovariectomized under tiletamine/zolazapamanesthetic (RaonBio Co., Ltd.). Prior to experimentation, mice were kept for a week and provided with water and sterile standard mouse chow ad libitum. They were housed in an air-conditioned animal room in a 12 h light/dark cycle at a temperature of 22 ± 1 °C and a humidity of 50 ± 10%. All experimental protocols involving the use of animals were conducted in accordance with National Institutes of Health guidelines and approved by the Committee on Animal Care of Kyung Hee University (KHUASP(SE)-18-030, approved on 20 September 2017).

Mice were randomly divided into 5 groups with 6 mice in each group as follows: (1) sham-operated control mice (Sham) received daily oral gavage of 0.85% NaCl, (2) OVX mice received daily oral gavage of 0.85% NaCl (OVX), (3) OVX mice were treated daily with 100 mg PE per kg body weight (b.w), (4) OVX mice were treated daily with 100 mg FPE per kg b.w, and (5) OVX mice received intraperitoneal (i.p) injections of $E_2$ (0.1 mg/kg b.w/day) every other day. Each treatment administration was performed for 12 weeks. At the end of treatment, the mice were sacrificed, and adequate serum was provided for CT analysis at the same time.

### *2.10. Micro-CT Bone Analysis*

The proximal and distal parts of the left tibia were scanned by micro-computer tomography (Micro-CT, Skyscan 1076, Billerica, MA, USA) to evaluate structural loss in

cortical and trabecular bone. Exposures were carried out at 50 kVp, 200 mA, and 360 ms. The micro-CT scans were analyzed with Comprehensive Tex Archive Network (CTAN) topographic reconstruction software. The trabecular bone volume represented the total trabecular bone within the total bone volume. By dividing the trabecular bone volume by the total volume, the bone volume percentage was calculated. The assessed cortical bone parameters were BMD, bone volume fraction (BV), mean polar moment of inertia (MMI), and cross-section thickness (Cs.Th). Trabecular bone parameters were used to assess the bone volume fraction (BV/TV), specific bone surface (BS/BV), trabecular thickness (Tb.Th), trabecular separation (Tb.Sp), trabecular number (Tb.N), trabecular bone pattern factor (Tb.Pf), structure model index (SMI), and BMD.

### *2.11. Serum Analysis*

At the end of the study, all animals fasted for 6 h, and blood was collected from the abdominalena cava under anesthesia with isoflurane. Blood was centrifuged at 12,000 rpm for 20 min at 4 °C to obtain serum. The serums were analyzed with enzyme-linked immunosorbent assay (ELISA) kits for RANKL, osteoprotegerin (OPG, R&D systems, Minneapolis, MN, USA), and osteocalcin (Alfa Aesar, Ward Hill, MA, USA). All ELISA procedures were performed according to the manufacturer's protocols.

### *2.12. Statistical Analysis*

Each experiment was repeated three or six times, and the results of the most representative experiment are shown. The results are expressed as the mean ± S.E.M and were analyzed using one-way ANOVA followed by Tukey's method (GraphPad Prism 5.0, San Diego, CA, USA). A statistical probability of $p < 0.05$ was considered significant.

## 3. Results and Discussion

### *3.1. Identification of Isoflavones in FPE*

*P. lobata* is used as herbal medicine and food [14,15]. *P. lobata* has demonstrated a variety of results related to osteoporosis [17–21]. Therefore, we evaluated the efficacy of fermented *P. lobata*, which contains various flavonoids, in the prevention of osteoporosis. In previous studies, it is confirmed that daidzein is converted to dihydrodaidzein and equol [27]. Furthermore, LC/MS qualitative analyses were performed to reveal other active components of FPE, especially isoflavones which are responsible for the strong inhibitory activities on osteoporosis. LC-MS analysis was conducted using the SCIEX Triple TOF 5600 (SCIEX) in positive ion mode. Using an HPLC system with a Kinetex F5 C18 column, the FPE were separated at a flow rate of 0.3 mL/min within 0 to 30 min. Each data set was processed with Analyst TF1.7 (SCIEX, Framingham, MA, USA) software. The total ion chromatograms (TIC) of FPE, including the name of each metabolite, retention time (RT), molecular formula, mass value, and accuracy, are shown in Figure 1. Particularly, puerarin, genistein, daidzein, calycosin, and equol are already known for their efficacy of anti-osteoporosis, respectively [28–32]. Therefore, it is believed that FPE, which includes various effective components, can be valuable candidate for anti-osteoporosis.

### *3.2. Effects of FPE on Proliferation, ALP Activities, and Gene Expression in MG 63 Cells*

Osteoporosis is a metabolic disease characterized by relatively low bone density and bone mass in comparison to healthy individuals [2–4]. It is also related to a homeostatic disproportion between bone formation and resorption. Even though the major cause of the disease is unclear, genetic, endocrinological, or nutritional factors are believed to be associated with osteoporosis.

The underlying mechanisms of the cellular effects of FPE have been studied in osteoblasts and osteoclasts. Osteoblasts and osteoclasts are specialized cells that are responsible for bone formation and resorption, respectively. The bone-forming cells, osteoblasts, synthesize and modulate the deposition and mineralization of the extracellular matrix of bone. Osteoclasts, on the other hand, are responsible for the resorption of aged bone.

Continuous stress leads to the inhibition of osteoblast activity and enhances osteoclast-mediated bone resorption, thus triggering a decrease in bone mass. Therefore, it can potentially lead to osteoporosis in the long term [33].

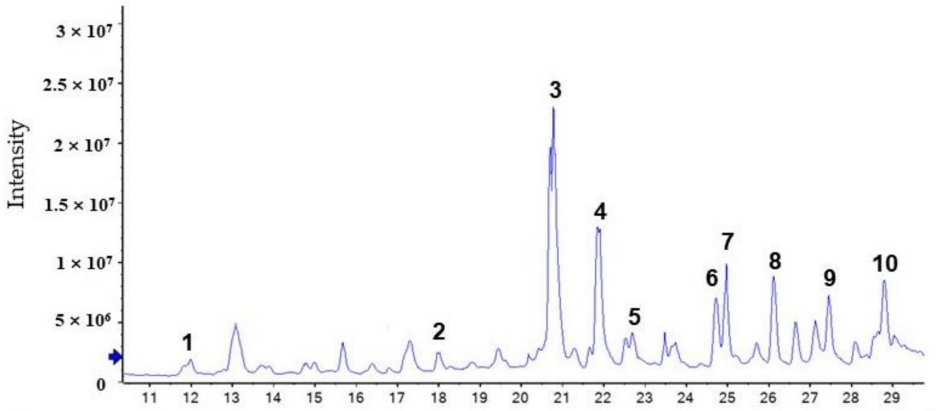


| No. | RT (min) | Compound | Molecular formula | Observed Mass (Da) | Expected Mass (Da) | Mass Accuracy (ppm) |
|---|---|---|---|---|---|---|
| 1 | 11.99 | puerarin | $C_{21}H_{20}O_9 + H$ | 417.1183 | 417.1186 | 0.623 |
| 2 | 17.96 | genistein | $C_{15}H_{10}O_5 + H$ | 271.0606 | 271.0607 | 0.184 |
| 3 | 20.78 | daidzein | $C_{15}H_{10}O_4 + H$ | 255.0657 | 255.0657 | 0.137 |
| 4 | 21.91 | prunetin | $C_{16}H_{12}O_5 + H$ | 285.0761 | 285.0763 | 0.702 |
| 5 | 22.71 | calycosin | $C_{16}H_{12}O_5 + H$ | 285.0762 | 285.0763 | 0.351 |
| 6 | 24.72 | 8-hydroxydaidzein | $C_{15}H_{10}O_5 + H$ | 271.0599 | 271.0607 | 2.767 |
| 7 | 25.02 | equol | $C_{15}H_{14}O_3 + H$ | 243.1019 | 243.1021 | 0.905 |
| 8 | 26.13 | trimethoxyflavone | $C_{18}H_{16}O_5 + H$ | 313.108 | 313.1076 | 1.278 |
| 9 | 27.45 | luteone | $C_{20}H_{18}O_6 + H$ | 355.1179 | 355.1182 | 0.746 |
| 10 | 28.80 | pratol | $C_{16}H_{12}O_4 + H$ | 269.0814 | 269.0814 | 0.056 |

**Figure 1.** HPLC-QTOF/MS chromatograms of FPE, and mass data in total ion chromatograms (TIC) scan mode. Analysis was carried out on a Kinetex F5 C18 column (2.6 µm, 2.1 × 100 mm) with gradient elution using solvents A (0.1% formic acid in water) and B (0.1% formic acid in acetonitrile). The elution gradients were as follows: 0–6 min, B 5%; 6–8 min, B 5–15%; 8–16 min, B 15–20%; 16–27 min, B 20–30%; 27–32 min, B 30–100%; and 30–34 min, B 100%. The flow rate was 300 µL/min, and the injection volume was 10 µL for each run. Mass detector settings were as follows: cone voltage 40 V; capillary 3.0 kV; source temperature 500 °C; cone gas flow 30 L/h; and desolvation gas flow at 800 L/h. The peaks of 1–10 were identified to be 10 metabolites.

The proliferative effects of FPE were evaluated in MG63 osteoblasts. PE and FPE significantly increased the proliferation rate (%) in a concentration-dependent manner (Figure 2A,B). FPE showed the ability to enhance the proliferation of cells as much as DHD (Figure 2C). As shown in Figure 2D, EQ, on the other hand, demonstrated a weaker proliferative ability than PE, FPE, and DHD. The proliferation rate of $E_2$ ($10^{-11}$ M) treated cell, the positive control, increased 114.8 ± 0.77% compared to control.

The alkaline phosphatase activity, a biological marker to indicate osteoblastic differentiation, was assessed in MG 63 osteoblasts. PE, FPE, DHD, EQ, and $E_2$ treatments were performed for 96 or 120 h each. ALP activities of PE and $E_2$ were significantly increased 96 h after treatment (Figure 3A). FPE showed a higher differentiation ability compared to PE and other compounds, including $E_2$, which was the positive control, after 120 h (Figure 3B).

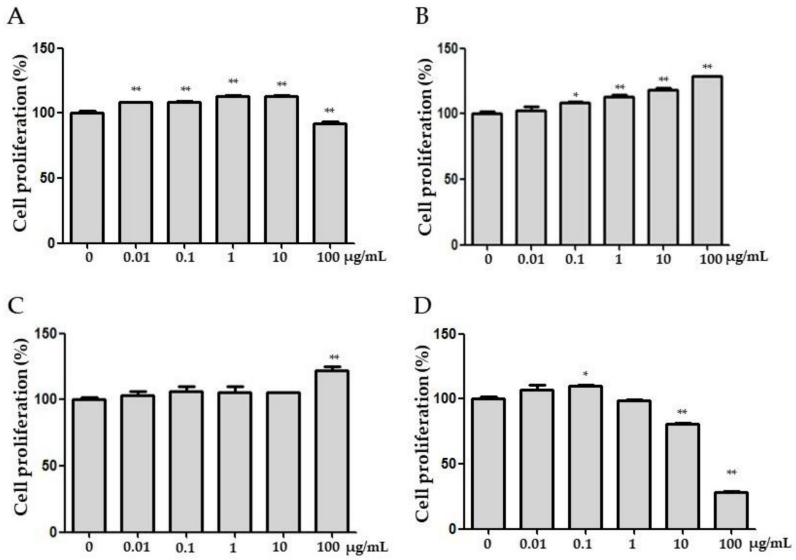


**Figure 2.** Proliferation activity in osteoblast MG63 cells. Effect of a variety concentration of (**A**) PE; (**B**) FPE; (**C**) DHD; (**D**) Equol on cell proliferation rate. * $p < 0.05$ compared to 0 μg/mL, ** $p < 0.01$ compared to 0 μg/mL. Data are means ± SEM of triplicates from one representative experiment.

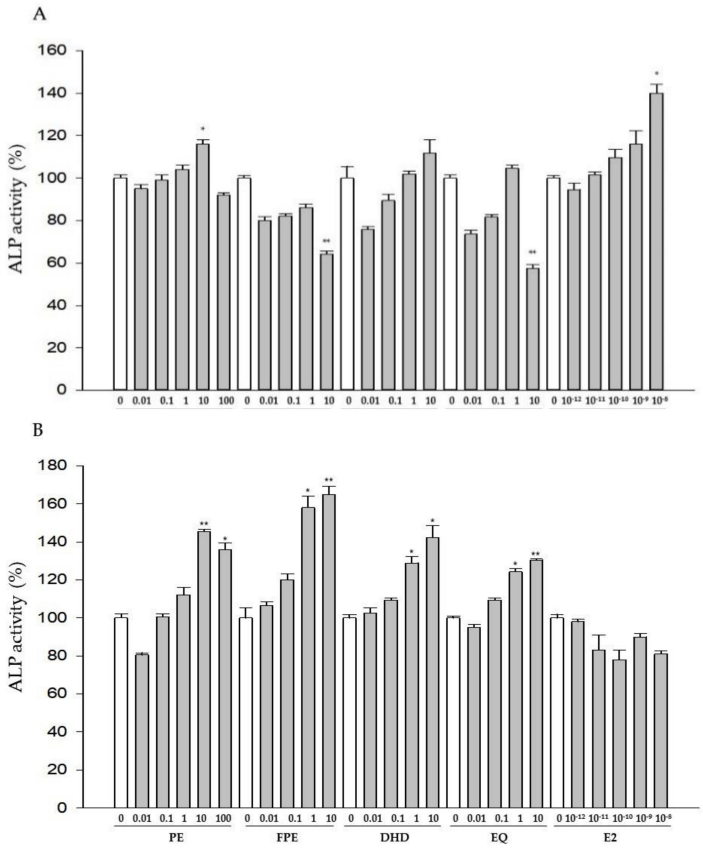


**Figure 3.** Effects of alkaline phosphate (ALP) activity in MG63 cells: (**A**) 96 h after treatment; (**B**) 120 h after treatment. PE: *Pueraria lobata* extract; FPE: fermented *Pueraria lobata* extract; DHD; dihydrodaidzein; EQ; equol. The results are expressed as a mean ± SEM ($n = 3$). * $p < 0.05$ compared to control, ** $p < 0.01$ compared to control.

The efficacy of FPE increased in a time-dependent manner. Consequently, it was demonstrated that the gene related to osteoblast differentiation was regulated by FPE.

FPE also increased calcium deposition in MG63 cells. For further exploration of the mechanisms of FPE's role in osteoblastic regulation, the markers of bone formation were evaluated in MG63 cells using RT-PCR. The levels of several bone formation biomarkers, OPG/RANKL, osteocalcin, osterix, and Runx2 mRNAs, were up-regulated by FPE treatment.

Osteoblasts synthesize and secrete OPG, which blocks the interaction between RANK and RANKL. Hence, the expression of OPG/RANKL plays a crucial role in modulating bone restoration. Additionally, OPG was able to block the interaction between RANKL and RANK, thus inhibiting osteoclastogenesis.

The efficacy of FPE in osteoblast differentiation was further elucidated by evaluating the expression of osteogenic differentiation mediator mRNA with RT-PCR. As shown in Figure 4, FPE increased the RANKL/OPG ratio in a concentration-dependent manner, but other genes (osteocalcin, osterix, and Runx2) did not have a significant effect.

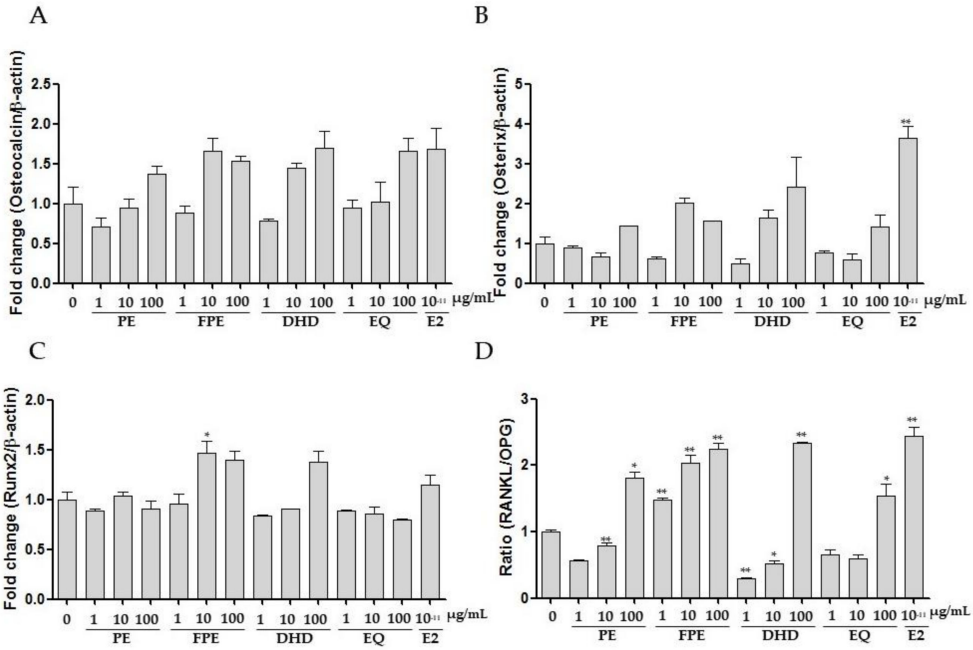


**Figure 4.** Expression of mRNA of osteogenic differentiation mediators, (**A**) osteocalcin/β-actin; (**B**) osterix; (**C**) Runx2; (**D**) RANKL/OPG, in MG 63 cells measured by real-time RT-PCR. The expression of β-actin was used as a loading control for RT-PCR. * $p < 0.05$ compared to normal controls and ** $p < 0.01$ compared to control. The results are expressed as a mean ± SEM ($n = 3$).

### *3.3. Effect of FPE on Osteoclast Differentiation in RAW 264.7 Cells*

The effects of FPE on RANKL/M-CSF-stimulated osteoclast differentiation in osteoclast precursor RAW 264.7 cells were then investigated. After 5 days of treatment of RANKL/M-CSF alone or with PE, FPE, DHD, EQ, and $E_2$, TRAP-positive MNC formation was examined, and TRAP-positive MNCs that contained more than three nuclei were counted as osteoclasts. RANKL/M-CSF treatment alone induced the formation of TRAP-positive multinuclear osteoclasts. RANKL/M-CSF-induced multinuclear osteoclast formation was significantly decreased following culturing with 100 μg/mL FPE (Figure 5).

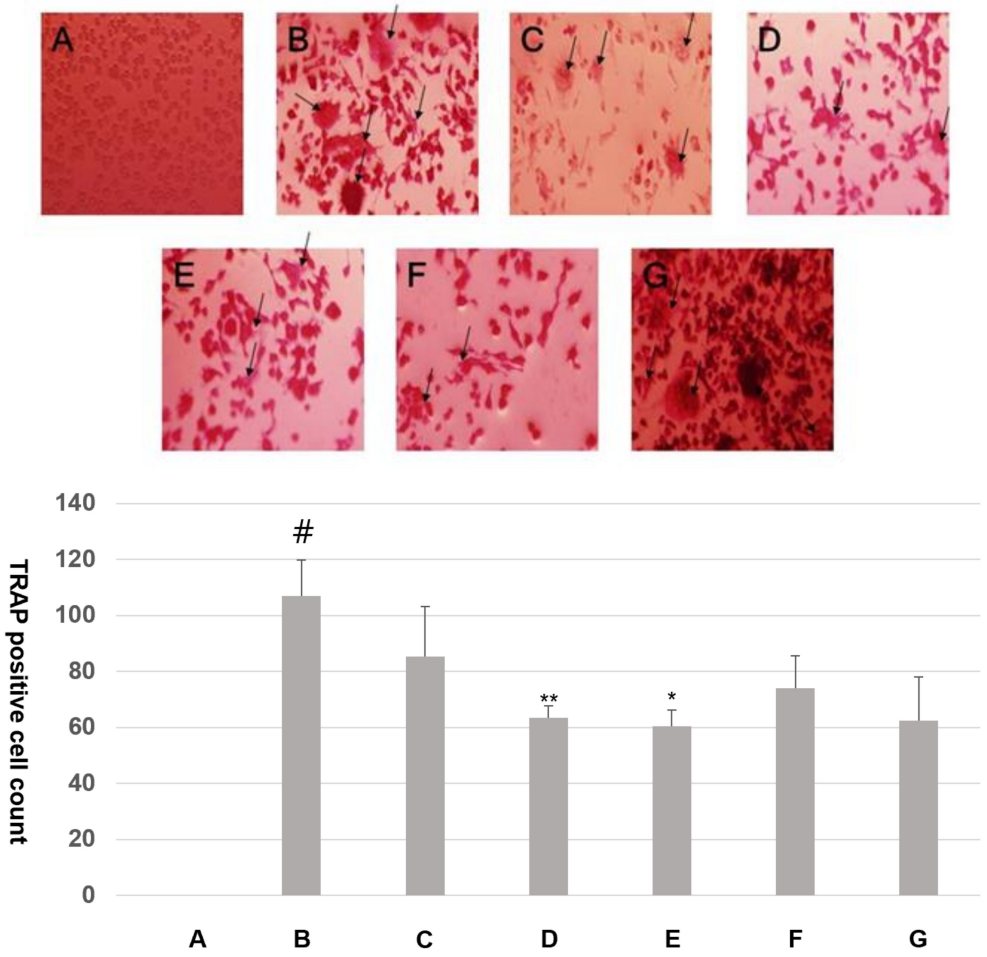


**Figure 5.** Osteoclast differentiation in osteoclast precursor RAW 264.7 cells: (**A**) Control; (**B**) RANKL 50 ng/mL + M-CSF 30 ng/mL; (**C**) RANKL/M-CSF + PE 100 μg/mL; (**D**) RANKL/M-CSF + FPE 100 μg/mL; (**E**) RANKL/M-CSF + DHD 10 μg/mL; (**F**) RANKL/M-CSF + EQ 10 μg/mL; (**G**) RANKL/M-CSF + $E_2$ $10^{-9}$ M 48 h after treatment. # $p < 0.01$ compared to control. * $p < 0.05$ compared to RANKL 50 ng/mL + M-CSF 30 ng/mL group. ** $p < 0.01$ compared to RANKL 50 ng/mL + M-CSF 30 ng/mL group.

### *3.4. Effects of FPE in OVX-Induced Mouse Model*

The OVX-induced mouse model has been widely used to investigate postmenopausal osteoporosis caused by estrogen deficiency [34]. An in vivo experiment using an OVX-induced bone loss mouse model was conducted to evaluate the anti-osteoporotic activity of FPE. As shown in Figure 6A, the body weight increase in the OVX group was higher compared with the sham operation group. On the other hand, mice given an oral administration of PE and FPE for 12 weeks after OVX showed a comparatively slower increase in body weight in comparison with the OVX group. Moreover, the decrease in uterus weight in the OVX group was lower than that in the sham operation group (Figure 6B). Mice that underwent intraperitoneal $E_2$ injection for 12 weeks after OVX showed a significant increase in uterus weight compared with the OVX group. However, mice given an oral administration of PE and FPE did not differ from sham-operated mice in terms of uterus weight. This result indicated that PE and FPE do not likely have the ability to stimulate or control hormone-dependent phenomena.

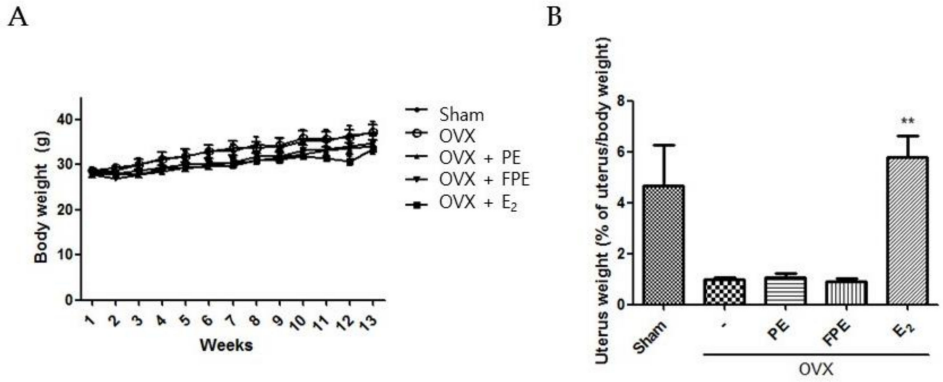


**Figure 6.** Effects of FPE on changes of body weight and uterus weight in OVX-induced mice. (**A**) Body weight was measured once a week; (**B**) at the end of the experiment, the uterus was removed and weighed. PE: *Pueraria lobata* extract; FPE: fermented *Pueraria lobata* extract. ** $p < 0.01$ compared to OVX induced control.

Deterioration of trabecular microarchitecture is apparent in the OVX mouse model [35]. We found that FPE prevented the deterioration of microstructural parameters in the distal femur of OVX model mice. An oral administration of FPE restored bone loss in the OVX mouse model.

To explore the structural characteristics affected by FPE, we scanned the tibia of each mouse (Figure 7A). The experimental and structural parameters for the entire cortical bone of the tibia, BV, BMD, MMI, and Cs. Th were measured and calculated in micro-CT images (Figure 7B). In the OVX group, BV, Cs. Th, MMI, and BMD did not change compared to the sham group. In addition, PE, FPE, and $E_2$ did not confer any significant change in the structural parameters.

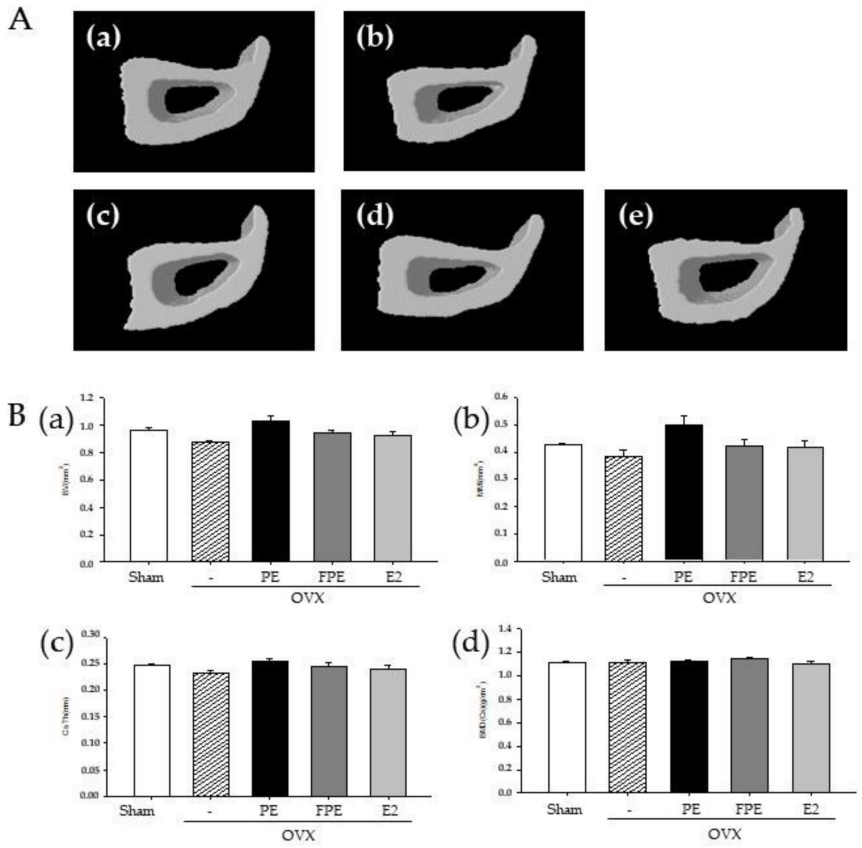


**Figure 7.** Micro-CT analysis of the cortical bone. (**A**) Micro-CT images of the cortical bone of the tibia;

(**a**) sham; (**b**) OVX; (**c**) OVX + PE 100 mg/kg; (**d**) OVX + FPE 100 mg/kg; (**e**) $E_2$; (**B**) (**a**) BV; (**b**) MMI; (**c**) Cs.Th; (**d**) BMD of OVX-induced mice treated PE, FPE, and $E_2$.

As illustrated in Figure 8A, OVX caused degradation of trabecular bone architecture compared to the sham group. However, treatment with PE and FPE retarded or recovered the destruction of femur trabecular bone in the OVX-induced bone loss mouse model. The protective effect on trabecular bone architecture was also clearly demonstrated by treatment with $E_2$, a positive control. In addition, BV/TV, Tb.Th, Tb.N, and BMD were lower, whereas trabecular separation, BS/BV, Tb.Th, Tb.Pf, and SMI were higher than the sham group (Figure 8B). In both the PE, FPE, and $E_2$ treatment groups, BV/TV, Tb.Th, Tb.N, and BMD were increased in sham-operated mice compared to those of the OVX group, while BS/BV, Tb.Sp, Tb.Pf, and SMI were decreased compared to those of the OVX group.

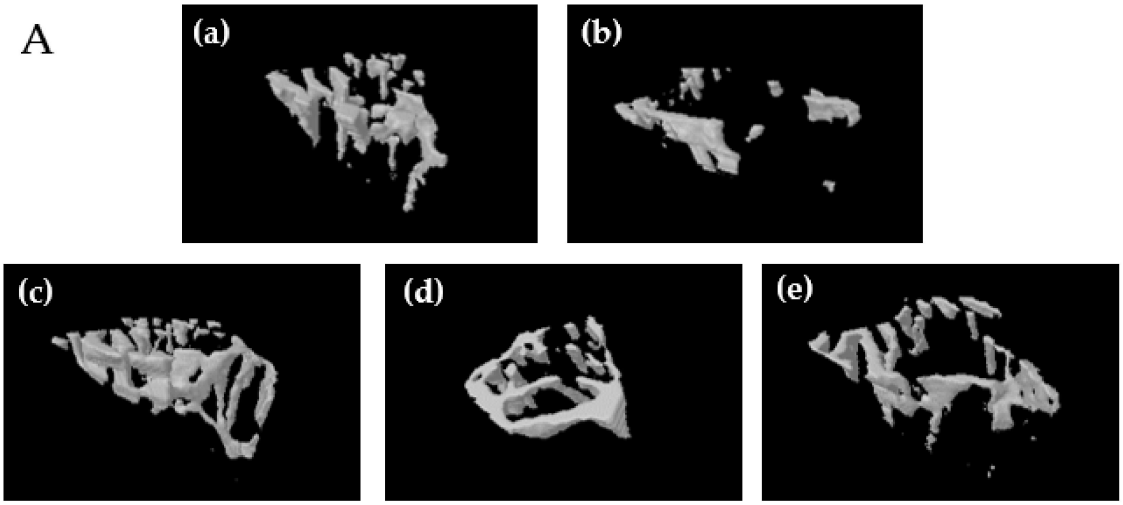


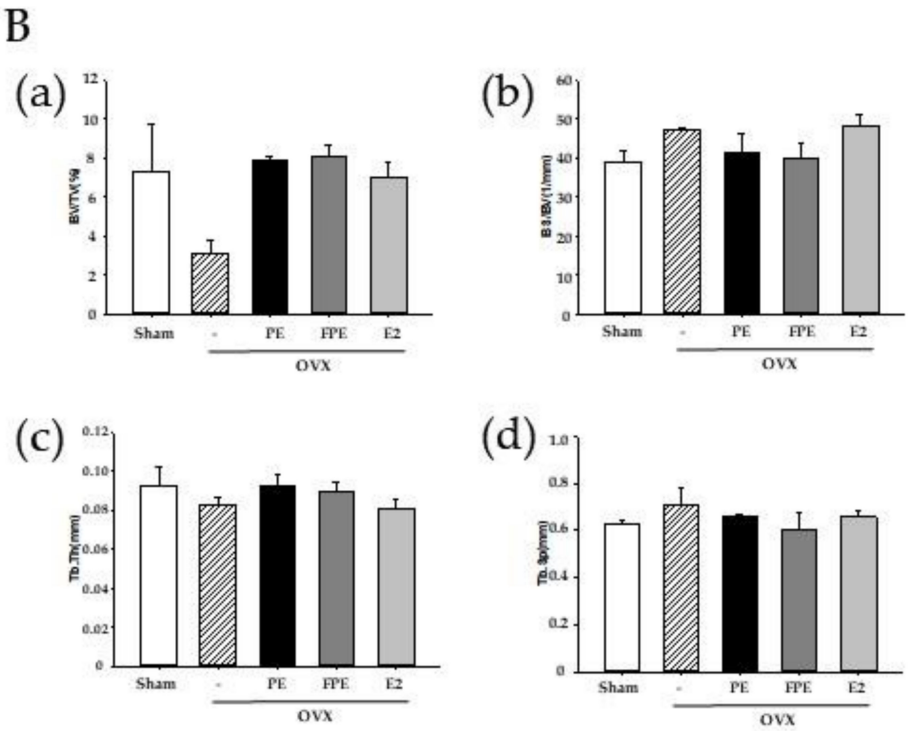


**Figure 8.** *Cont.*

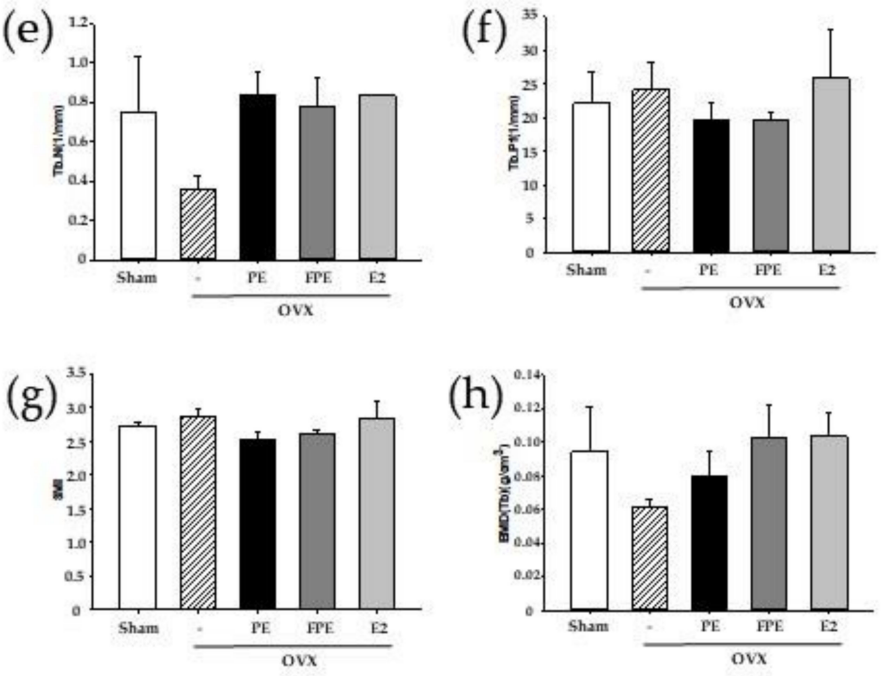


**Figure 8.** Micro-CT analysis of the trabecular bone. (**A**) Micro-CT images of the trabecular bone of the femur; (**a**) sham; (**b**) OVX; (**c**) OVX + PE 100 mg/kg; (**d**) OVX + FPE 100 mg/kg; (**e**) $E_2$; (**B**) (**a**) BV/TV; (**b**) BS/BV; (**c**) Tb.Th; (**d**) Tb.Sp; (**e**) Tb.N; (**f**) Tb.Pf; (**g**) SMI; (**h**) BMD of OVX-induced mice treated PE, FPE, and $E_2$.

These results suggest that FPE was effective in preserving bone mass as well as in restoring the deterioration of bone microarchitecture associated with OVX mice. Analyses of the serum levels of OPG/RANKL and osteocalcin, biomarkers of bone resorption, were shown to be significantly higher than those of the sham group. In the present study, PE and FPE showed protective efficacy against OVX-induced osteoporosis. It is hypothesized that the FPE could be effective in inhibiting the bone resorption process. Since the balance between the RANKL and OPG produced by osteoblasts is critical for osteoclast regulation, we determined serum levels of RANKL and OPG by ELISA (Figure 9). In the OVX group, serum levels of RANKL were decreased, whereas OPG was decreased compared to that of the sham group. Our results indicate that FPE treatment significantly increased the level of OPG; however, it did not affect the level of RANKL. As a consequence, the RANKL/OPG ratio was significantly decreased by FPE treatment. On the other hand, osteocalcin, which is the most abundant protein in bone matrix after its synthesis by osteoblasts, increased dramatically following FPE treatment compared to other groups. This suggests that FPE most likely prevented bone loss through decreased bone turnover.

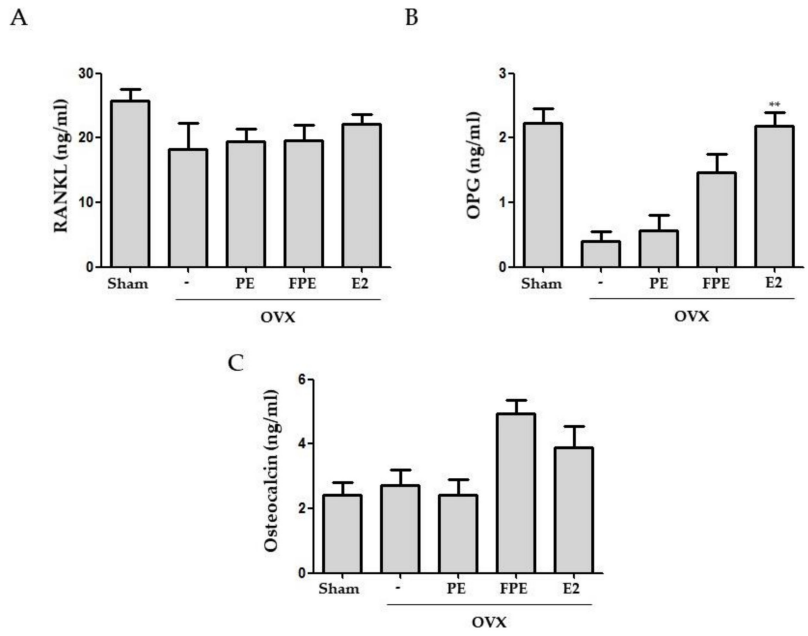


**Figure 9.** Serum levels of (**A**) RANKL, (**B**) OPG, and (**C**) osteocalcin measured by ELISA.

## 4. Conclusions

The present study suggests that FPE has anti-osteoporosis efficacy both in vitro and in vivo. In vitro studies indicated that FPE tends to have more regulatory effects on MG63 cells than PE and the positive controls. In the OVX-induced mouse model, FPE was effective in preserving bone mass and preventing the deterioration of microstructural parameters. These data provide a pharmacological basis on which FPE could be considered a therapeutic compound to prevent osteoporotic bone loss. Further research is needed to ensure the safety, specificity, and efficacy of FPE to develop its therapeutic potential. To support the present study, additional experiments such as an inhibition on osteoclast activity or mechanism analysis on RANKL-induced RAW 264.7 cells are considered. In addition, more high-quality clinical research is necessary to provide evidence for FPE as an effective anti-osteoporotic candidate.

**Author Contributions:** Conceptualization, J.E.K. and S.C.K.; methodology, J.E.K. and Y.-G.L.; software, Y.-G.L., T.K.; validation, S.Y.K., H.-J.L.; formal analysis, J.E.K.; investigation, J.E.K. and S.Y.K.; resources, J.E.K.; data curation, T.K.; writing—original draft preparation, J.E.K. and S.Y.K.; writing—review and editing, J.E.K., S.Y.K. and S.C.K.; visualization, H.-J.L. and T.K.; supervision, Y.-G.L. and S.C.K.; project administration, S.C.K. All authors have read and agreed to the published version of the manuscript.

**Funding:** This research received no external funding.

**Institutional Review Board Statement:** The study was conducted according to the guidelines of the Declaration of Helsinki and approved in accordance with the current ethical regulations for anima care and use at Kyung Hee University (KHUASP(SE)-18-030, approved on 20 September 2017.

**Data Availability Statement:** Data are contained within the article.

**Conflicts of Interest:** The authors declare no conflict of interest.

## References

1. Magee, P.J. Is equol production beneficial to health? *Proc. Nutr. Soc.* **2011**, *70*, 10–18. [CrossRef] [PubMed]
2. Alexander, J.M.; Bab, I.; Fish, S.; Muller, R.; Uchiyama, T.; Gronowicz, G.; Nahounou, M.; Zhao, Q.; White, D.W.; Chorev, M.; et al. Human parathyroid hormone 1–34 reverses bone loss in ovariectomized mice. *J. Bone Miner. Res.* **2001**, *16*, 1665–1673. [CrossRef]
3. Chung, H.J.; Cho, L.; Shin, J.S.; Lee, J.; Ha, I.H.; Park, H.J.; Lee, S.K. Effects of JSOG-6 on protection against bone loss in ovariectomized mice through regulation of osteoblast differentiation and osteoclast formation. *BMC Complement. Altern. Med.* **2014**, *14*, 184. [CrossRef] [PubMed]

4. Raisz, L.G. Pathogenesis of osteoporosis: Concepts, conflicts, and prospects. *J. Clin. Investig.* **2005**, *115*, 3318–3325. [CrossRef] [PubMed]
5. Fu, Y.S.; Lu, C.H.; Chu, K.A.; Yeh, C.C.; Chiang, T.L.; Ko, T.L.; Chiu, M.M.; Chen, C.F. Xenograft of Human Umbilical Mesenchymal Stem Cells from Wharton's Jelly Differentiating into Osteocytes and Reducing Osteoclast Activity Reverses Osteoporosis in Ovariectomized Rats. *Cell Transplant.* **2018**, *27*, 194–208. [CrossRef]
6. Seeman, E. Invited Review: Pathogenesis of osteoporosis. *J. Appl. Physiol.* **2003**, *95*, 2142–2151. [CrossRef]
7. Kang, H.; Aryal, A.C.S.; Marini, J.C. Osteogenesis imperfecta: New genes reveal novel mechanisms in bone dysplasia. *Transl. Res.* **2017**, *181*, 27–48. [CrossRef]
8. Meunier, P.J. Hyperthyroidism and osteoporosis. *Ann. Endocrinol.* **1995**, *56*, 57–59. [PubMed]
9. Redlich, K.; Smolen, J.S. Inflammatory bone loss: Pathogenesis and therapeutic intervention. *Nat. Rev. Drug Discov.* **2012**, *11*, 234–250. [CrossRef] [PubMed]
10. Zhang, G.; Qin, L.; Hung, W.Y.; Shi, Y.Y.; Leung, P.C.; Yeung, H.Y.; Leung, K.S. Flavonoids derived from herbal Epimedium Brevicornum Maxim prevent OVX-induced osteoporosis in rats independent of its enhancement in intestinal calcium absorption. *Bone* **2006**, *38*, 818–825. [CrossRef] [PubMed]
11. Dionyssiotis, Y.; Skarantavos, G.; Papagelopoulos, P. Modern rehabilitation in osteoporosis, falls, and fractures. *Clin. Med. Insights Arthritis Musculoskelet. Disord.* **2014**, *7*, 33–40. [CrossRef] [PubMed]
12. Das, S.; Crockett, J.C. Osteoporosis—A current view of pharmacological prevention and treatment. *Drug Des. Dev. Ther.* **2013**, *7*, 435–448. [CrossRef]
13. Chow, T.H.; Lee, B.Y.; Ang, A.B.F.; Cheung, V.Y.K.; Ho, M.M.C.; Takemura, S. The effect of Chinese martial arts Tai Chi Chuan on prevention of osteoporosis: A systematic review. *J. Orthop. Transl.* **2018**, *12*, 74–84. [CrossRef] [PubMed]
14. Zheng, X.; Lee, S.K.; Chun, O.K. Soy Isoflavones and Osteoporotic Bone Loss: A Review with an Emphasis on Modulation of Bone Remodeling. *J. Med. Food* **2016**, *19*, 1–14. [CrossRef]
15. Hickman, J.E.; Wu, S.; Mickley, L.J.; Lerdau, M.T. Kudzu (*Pueraria montana*) invasion doubles emissions of nitric oxide and increases ozone pollution. *Proc. Natl. Acad. Sci. USA* **2010**, *107*, 10115–10119. [CrossRef] [PubMed]
16. Koirala, P.; Seong, S.H.; Jung, H.A.; Choi, J.S. Comparative molecular docking studies of lupeol and lupenone isolated from Pueraria lobata that inhibits BACE1: Probable remedies for Alzheimer's disease. *Asian Pac. J. Trop. Med.* **2017**, *10*, 1117–1122. [CrossRef] [PubMed]
17. Keung, W.M.; Vallee, B.L. Kudzu root: An ancient Chinese source of modern antidipsotropic agents. *Phytochemistry* **1998**, *47*, 499–506. [CrossRef]
18. Gao, Y.; Wang, X.; He, C. An isoflavonoid-enriched extract from Pueraria lobata (kudzu) root protects human umbilical vein endothelial cells against oxidative stress induced apoptosis. *J. Ethnopharmacol.* **2016**, *193*, 524–530. [CrossRef]
19. Jin, S.E.; Son, Y.K.; Min, B.S.; Jung, H.A.; Choi, J.S. Anti-inflammatory and antioxidant activities of constituents isolated from Pueraria lobata roots. *Arch. Pharm. Res.* **2012**, *35*, 823–837. [CrossRef]
20. Seong, S.H.; Roy, A.; Jung, H.A.; Jung, H.J.; Choi, J.S. Protein tyrosine phosphatase 1B and alpha-glucosidase inhibitory activities of Pueraria lobata root and its constituents. *J. Ethnopharmacol.* **2016**, *194*, 706–716. [CrossRef]
21. Cheung, D.W.; Koon, C.M.; Wat, E.; Ko, C.H.; Chan, J.Y.; Yew, D.T.; Leung, P.C.; Chan, W.Y.; Lau, C.B.; Fung, K.P. A herbal formula containing roots of Salvia miltiorrhiza (Danshen) and Pueraria lobata (Gegen) inhibits inflammatory mediators in LPS-stimulated RAW 264.7 macrophages through inhibition of nuclear factor kappaB (NFkappaB) pathway. *J. Ethnopharmacol.* **2013**, *145*, 776–783. [CrossRef] [PubMed]
22. Park, K.H.; Gu, D.R.; Jin, S.H.; Yoon, C.S.; Ko, W.; Kim, Y.C.; Lee, S.H. Pueraria lobate Inhibits RANKL-Mediated Osteoclastogenesis Via Downregulation of CREB/PGC1beta/c-Fos/NFATc1 Signaling. *Am. J. Chin. Med.* **2017**, *45*, 1725–1744. [CrossRef] [PubMed]
23. Huh, J.E.; Yang, H.R.; Park, D.S.; Choi, D.Y.; Baek, Y.H.; Cho, E.M.; Cho, Y.J.; Kang-Il, K.; Kim, D.Y.; Lee, J.D. Puerariae radix promotes differentiation and mineralization in human osteoblast-like SaOS-2 cells. *J. Ethnopharmacol.* **2006**, *104*, 345–350. [CrossRef] [PubMed]
24. Hessle, C.; Hanson, L.A.; Wold, A.E. Lactobacilli from human gastrointestinal mucosa are strong stimulators of IL-12 production. *Clin. Exp. Immunol.* **1999**, *116*, 276–282. [CrossRef]
25. Molin, G.; Jeppsson, B.; Johansson, M.L.; Ahrne, S.; Nobaek, S.; Stahl, M.; Bengmark, S. Numerical taxonomy of Lactobacillus spp. associated with healthy and diseased mucosa of the human intestines. *J. Appl. Bacteriol.* **1993**, *74*, 314–323. [CrossRef]
26. Kwon, J.E.; Lim, J.; Bang, I.; Kim, I.; Kim, D.; Kang, S.C. Fermentation product with new equol-producing Lactobacillus paracasei as a probiotic-like product candidate for prevention of skin and intestinal disorder. *J. Sci. Food Agric.* **2019**, *99*, 4200–4210. [CrossRef]
27. Matthies, A.; Loh, G.; Blaut, M.; Braune, A. Daidzein and Genistein Are Converted to Equol and 5-Hydroxy-Equol by Human Intestinal Slackia isoflavoniconvertens in Gnotobiotic Rats. *Nutr. J.* **2012**, *142*, 40–46. [CrossRef]
28. Xiao, L.; Zhong, M.; Huang, Y. Puerarin alleviates osteoporosis in the ovariectomy-induced mice by suppressing osteoclastogenesis via inhibition of TRAF6/ROS-dependent MAPK/NF-κB signaling pathways. *Aging* **2020**, *12*, 21706–21729. [CrossRef]
29. An, J.; Yang, H.; Zhang, Q. Natural products for treatment of osteoporosis: The effects and mechanisms on promoting osteoblast-mediated bone formation. *Life Sci.* **2016**, *147*, 46–58. [CrossRef]

30. Zou, S.E.; Zhang, S.F.; Zhang, R.; Zhang, J. Role of the cross-talk between estrogen receptors and peroxisome proliferator-activated receptor gamma in daidzein's prevention and treatment of osteoporosis in ovariectomized rats. *Zhonghua Yi Xue Za Zhi* **2009**, *89*, 2972–2975. [PubMed]
31. Li, N.; Tu, Y.; Shen, Y.; Qin, Y.; Lei, C.; Liu, X. Calycosin attenuates osteoporosis and regulates the expression of OPG/RANKL in ovariectomized rats via MAPK signaling. *Pharmazie* **2016**, *71*, 607–612. [CrossRef]
32. Fujioka, M.; Uehara, M.; Wu, J. Equol, a metabolite of daidzein, inhibits bone loss in ovariectomized mice. *J. Nutr.* **2004**, *134*, 2623–2627. [CrossRef] [PubMed]
33. Katagiri, T.; Takahashi, N. Regulatory mechanisms of osteoblast and osteoclast differentiation. *Oral. Dis.* **2002**, *8*, 147–159. [CrossRef] [PubMed]
34. Frolik, C.A.; Bryant, H.U.; Black, E.C.; Magee, D.E.; Chandrasekhar, S. Time-dependent changes in biochemical bone markers and serum cholesterol in ovariectomized rats: Effects of raloxifene HCl, tamoxifen, estrogen, and alendronate. *Bone* **1996**, *18*, 621–627. [CrossRef]
35. Cano, A.; Dapia, S.; Noguera, I.; Pineda, B.; Hermenegildo, C.; del Val, R.; Caeiro, J.R.; Garcia-Perez, M.A. Comparative effects of 17beta-estradiol, raloxifene and genistein on bone 3D microarchitecture and volumetric bone mineral density in the ovariectomized mice. *Osteoporos. Int.* **2008**, *19*, 793–800. [CrossRef]